PHYSICS OF HEAVY QUARKS FROM LATTICE QCD

Apoorva Patel
CTS and SERC, Indian Institute of Science, Bangalore-560012

Abstract

In the last few years, lattice QCD has made a dramatic progress in understanding the physics of hadrons containing heavy quarks, from the first principle. This review summarises the major achievements.

I. INTRODUCTION

Heavy quarks play a dominant role in the understanding of the weak interactions as well as of what may lie beyond the standard model. Since quarks are always bound into hadrons, and we do not understand the strong interactions rigorously, the results of these phenomena are often expressed in terms of non-perturbative parameters (also called matrix elements) that reflect our knowledge/ignorance of the strong interaction effects. Lattice QCD offers the best route to a non-perturbative determination of these parameters.

The field of lattice gauge theories has nowadays achieved a maturity level where statistical errors are beaten down enough to expose systematic effects. This control over systematic effects has helped reliable extraction of matrix elements that allow us to test the Standard Model. In fact the results of these numerical experiments are now acknowledged by the Particle Data Group [1]. What I present below are excerpts from results of many lattice QCD calculations; more details can be found in the proceedings of the annual lattice field theory conferences [2, 3].

Lattice QCD simulations of hadrons containing heavy quarks provide a testing ground for many new ideas. The heavy hadrons are smaller than the light hadrons, and hence less susceptible to effects of finite lattice volume and dynamical quarks. (Typical lattice size in simulations nowadays is $1.5-2$ fm.) Their nonrelativistic nature allows an easy comparison of the results with those from phenomenological quark potential models. Moreover, the results do not suffer from the uncertainties of chiral extrapolations.

Three different formalisms for heavy quarks have been used in lattice QCD to get at the properties of heavy hadrons: (1) static, (2) non-relativistic (NRQCD), (3) conventional.

$$L_1 = \overline{Q} v_\mu D^\mu Q \tag{1}$$

$$L_2 = \overline{Q}[D^0 - \frac{1}{2M}\vec{D}^2 + \frac{c_1}{2M}\vec{\sigma}\cdot\vec{B} + \mathcal{O}(\frac{1}{M^2})]Q \tag{2}$$

$$L_3 = \overline{q}(\not{D} + M)q \tag{3}$$

Here Q refers to 2−component heavy quark fields, defined so as to remove the static mass M from the Lagrangian (otherwise M would appear as an additive constant). The field q contains both particle and anti-particle components, and M cannot be removed in that case. The coefficient c_1 has to be non-perturbatively determined by a matching between NRQCD and conventional formalisms.

In the static case, the 4−velocity of the heavy quark is a constant of motion, and the calculations are often carried out in the rest frame. The formalism is meaningful when the hadron has only one heavy quark, and the results provide the limiting behaviour as $M \to \infty$. The NRQCD formalism is organised in powers of M^{-1} for hadrons having only one heavy quark, and in powers of $v \sim p/M \sim \alpha_s(p)$ for hadrons having more heavy quarks [4].

The lattice momentum cutoff in typical simulations nowadays is $\pi/a \sim 5 - 10$ GeV. The NRQCD approach is useful for $Ma > 1$. With the inclusion of $\mathcal{O}(M^{-1})$ terms, L_2 works well for b−quarks and can be extrapolated to the case of c−quark. The conventional approach requires $Ma < 1$. It works reasonably for c−quarks, and can be extrapolated to heavier masses.

A good consistency check on the methods is that the NRQCD and the conventional results agree in the region between m_b and m_c. This comparison requires various M−dependent renormalisations to justify the extrapolations in the quark mass, but at the end we have continuous functional behaviour for the quantities measured.

There are many technical details involved in converting lattice results to numbers useful for phenomenology. The techniques are sophisticated, and the caveats should be kept in mind, instead of blindly using the numbers in phenomenological analyses. I only mention these without elaboration:

- Both the action and the operators are improved, using higher order terms in a and M^{-1} to cut down discretisation errors. The creation and annihilation operators for the asymptotic states are smeared to increase overlap with the desired wavefunctions.

- The lattice perturbation theory is not well-behaved in terms of the bare coupling. Rather one needs to express the results in terms of the renormalised coupling that is extracted from the simulation itself. A poor man's choice is "tadpole-improved" perturbation theory. With a non-perturbative cutoff, the lattice results are unambiguous, but renormalon ambiguities appear when converting them to a continuum scheme such as $\overline{MS}$.

- The symmetries of the lattice theory are only a subset of the continuum ones. This makes renormalisation and mixing of the lattice operators more complicated than in the continuum. In principle, all the renormalisation constants should be determined through non-perturbative definitions. In practice, it turns out that finite and logarithmic renormalisations (e.g. dim≤ 4 operators such as quark bilinears) can be well estimated using the renormalised perturbation theory. Power law divergences (e.g. dim> 4 operators mixing with lower dimension operators), however, have to be eliminated using non-perturbative subtractions based on Ward identities.

- A majority of lattice results, and certainly the ones where all the errors are well under control, are obtained in the quenched approximation ignoring the effects of dynamical quarks. This approximation violates the unitarity of the theory and unphysical singularities appear in the chiral limit. Simulation results indicate that these violations, however, are not serious for typical simulations carried out with the light quark about as heavy as the strange quark. For certain quantities, results including two or four flavours of dynamical quarks have become available. These are combined with the quenched (i.e. $n_f = 0$) values to obtain physically relevant numbers (i.e. $n_f = 3$).

- Specific scaling forms are used to extrapolate the results to the infinite volume, continuum and chiral limits. Algorithms for simulation of the path integral and for calculation of the quark propagator in a background gluon field keep on getting revised. Parametrisation of the highly correlated lattice data needs careful fitting procedures.

II. PROPERTIES OF HEAVY-HEAVY MESONS

Spectroscopy of heavy quarkonia (Upsilon, Charmonium and B_c) is the simplest test of lattice simulations. There are two bare parameters: the coupling and the heavy quark mass. Effects of light quarks appear only through vacuum polarisation loops. NRQCD simulations directly extract the level splittings, and the lattice cutoff is determined (in GeV) by assigning one of the splittings its physical value. The splittings are largely insensitive to the precise value of M, which keeps systematic errors under control. A remarkable feature of the results is that many of them have been obtained on rather coarse lattices using improved actions.

Fig.1 shows how well the lowest spin-averaged states of the Upsilon spectrum can be reproduced [5]. A closer look reveals that the effects of light dynamical quarks shift the numbers closer to their experimental values. The Upsilon hyperfine splittings, shown in Fig.2, are more sensitive to the details of the lattice action: quenching tends to underestimate them, and accurate values are needed for M and c_1 (which undergoes substantial renormalisation).

Results for Charmonium and B_c (not yet discovered) spectra are not as impressive. The main difficulty is that the quarks are more relativistic and higher order terms in the NRQCD expansion are needed to keep the systematic errors under control. The results are still phenomenologically useful and can be used to tune quark models. An example of Coulomb gauge wavefunctions for Charmonium states is shown in Fig.3 [6].

Calculations of heavy-light hadron masses suffer from the additional uncertainty of extrapolating the light quark mass to the chiral limit. Results are again best expressed as level splittings. Reasonable values are found for $B_s - B$, $\Lambda_b - B$ and $\Sigma_b - \Lambda_b$ splittings. Hyperfine splittings (e.g. $B^* - B$ and $\Sigma_b^* - \Sigma_b$), however, are typically underestimated and require more care.

First results for annihilation decays of quarkonia have recently become available [7]. Annihilation decay rates, $\Gamma(Q\overline{Q} \to \mathit{light\ hadrons}, \gamma\gamma, l^+l^-)$, can be expressed as a power series in M^{-1}, with each term factorised into a short distance perturbative coefficient and a non-perturbative hadronic matrix element of 4−fermion operators [8]. In the vacuum saturation approximation (VSA), the "colour singlet" combinations can be written in terms of

quarkonium wave functions at the origin and their derivatives. The "colour octet" contributions measure the $Q\overline{Q}g$ component in the $P-$wave states. The numerical results are in reasonable accord with the VSA and the experimental data.

III. THE QCD RUNNING COUPLING

To verify that QCD is indeed the theory of the strong interactions, it must be demonstrated that perturbative and non-perturbative determinations of the coupling α_s agree. The former is typically extracted from experimental results of high energy processes. The latter can be evaluated on the lattice from low energy hadronic properties. To this end, several non-perturbative definitions of α_s have been employed (note that $\alpha_{\overline{MS}}$ does not exist outside perturbation theory):

$$\alpha_{q\overline{q}}(q=\frac{1}{r}) \;=\; C_F^{-1} r^2 F(r) \qquad \stackrel{q\to 0}{\longrightarrow} \; \infty \tag{4}$$

$$\alpha_{SF}(q=\frac{1}{L}) \;\propto\; [\frac{\partial}{\partial\eta}\ln Z(L,\eta)]_{\eta=0} \qquad \stackrel{q\to 0}{\longrightarrow} \; 0 \tag{5}$$

$$\alpha_{TP}(q=\frac{1}{L}) \;\propto\; \frac{\langle P_x(0)P_x(L)\rangle}{\langle P_z(0)P_z(L)\rangle} \qquad \stackrel{q\to 0}{\longrightarrow} \; \text{constant} \tag{6}$$

$$\alpha_P(q=\frac{3.4}{a}) \;=\; -\frac{3}{4\pi}\frac{\ln\langle W_{1\times 1}\rangle}{(1-(1.19+0.07n_f)\alpha_P)} \qquad \stackrel{q\to 0}{\longrightarrow} \; \infty \tag{7}$$

The infrared behaviour of these definitions differ, as indicated above, but they should all come together towards the ultraviolet end. Strictly speaking, with a non-perturbative regulator, scaling is exact only on the critical surface. Away from $g=0$, scaling holds only upto a certain tolerance level, and different definitions of α_s help quantify this tolerance level. A comparison of g^2_{SF} and g^2_{TP} for the pure gauge $SU(2)$ theory, shown in Fig.4 [9], gives us faith to use perturbative scaling in the actual region of simulations.

Having demonstrated scaling, the lattice results can be converted into a value for $\alpha_{\overline{MS}}(M_Z)$. The common procedure is to use the spectrum results for quarkonia to determine α_P at a specific value of the cutoff, and then use perturbation theory to convert it into $\alpha_{\overline{MS}}$. Given that $\alpha_s = \mathcal{O}(0.1)$, a precision of $\mathcal{O}(1\%)$ requires $2-$loop perturbative matching. Determinations of α_s from different spectral quantities need not agree with each-other, when the number of dynamical quarks is unphysical. It is reassuring to see, as illustrated in Fig.5 [10], that they indeed converge when extrapolated to $n_f = 3$. Results obtained by various groups and their extrapolations to $n_f = 3$ are displayed in Fig.6 [5]; they typically lie at the lower edge of the band of values from non-lattice determinations.

There is yet another step in converting lattice numbers to a physical $\alpha_{\overline{MS}}(M_Z)$. The dynamical quarks included in lattice simulations are much heavier than the physical u and d quarks, and do not correctly reproduce the effects of pion loops. Chiral symmetry breaking in QCD implies that extrapolation of spectral quantities to the chiral limit be linear in the quark mass [11], in contrast to quadratic dependence seen in weak coupling perturbation theory. The final result is [5]

$$\alpha_{\overline{MS}}(M_Z) \;=\; 0.117(1)(1)(2) \quad , \tag{8}$$

where the first error combines statistical and discretisation uncertainties, the second is due to m_{dyn}, and the third comes from perturbative conversions.

IV. PROPERTIES OF HEAVY-LIGHT PSEUDOSCALARS

The pseudoscalar decay constant is a phenomenologically important parameter. Though its calculation on the lattice is straightforward, the number has remained hard to pin down due to its substantial mass dependence—Fig.7 [12] shows the extent of $\mathcal{O}(M^{-1})$ corrections to the static limit. Exploiting the freedom that the various $\mathcal{O}(M^{-1})$ contributions can be selectively extracted from lattice simulations, the high sensitivity of f_{Qq} to quark mass has been traced down to the large heavy quark kinetic energy [13]. Fig.8 [12] shows the extrapolation of f_B values to the continuum, and also indicates that dynamical quarks would increase f_B somewhat. Overall it is safe to quote [12, 14]

$$f_B \;=\; 180(20)\ \text{MeV} \quad (\text{with } f_\pi = 132\ \text{MeV}) \quad . \tag{9}$$

The ratios of decay constants are more stable as several correlated systematic errors cancel, and the results are [12, 14]:

$$f_B/f_D \;\approx\; 0.85 \quad , \quad f_{B_s}/f_B \;\approx\; 1.10 \quad , \quad f_{D_s}/f_D \;\approx\; 1.10 \quad , \tag{10}$$

all with errors of about 5%.

Lattice calculations have also estimated several bound state parameters often used in $B-$physics phenomenology. In absence of any asymptotic quark states in QCD, these are defined through behaviour of lattice quark propagators in the Landau gauge. To quote [15]: the $B-$meson binding energy $\overline{\Lambda} = 180(30)$ MeV, the $\overline{MS}$ running quark mass $m_b(m_b) = 4.15(20)$ GeV, the heavy quark kinetic energy in $B-$meson $\lambda_1 = 0.1(1)$ GeV^2.

The $B-$parameter characterising $B - \overline{B}$ mixing is another useful quantity. In the effective theory below m_b, it has no anomalous dimension at 1−loop. It can be easily seen, at least at strong coupling, that the deviation of B_B from one is $\mathcal{O}(M^{-1}, N_c^{-2})$. Indeed different lattice calculations confirm that $B_B(m_b) = 0.90(5)$ [16]. Dynamical quarks do not seem to have substantial effect on B_B. Increasing the light quark mass increases B_B slightly, so that $B_{bs} > B_{bd}$. Conversion of the lattice B_B to the RG-invariant value used in continuum analyses is rather uncertain: $\hat{B}_B = 1.3(2)$.

V. FORM FACTORS OF HEAVY-LIGHT HADRONS

The spin-flavour symmetries of heavy quarks reduce form factors of heavy-light hadrons to Isgur-Wise functions [17]. Matrix elements of the charge operators (i.e. $\vec{p}_i = \vec{p}_f$) determine the form factor normalisations, and provide scaling rules for their $M-$dependence. In the heavy quark effective theory, the charge operators act in the rest frame, and hence constrain the form factors at $q^2 = q^2_{\rm max}$. On the other hand, the charge operators correspond to $q^2 = 0$ in the lightcone frame, and thus the lightcone sum rules constrain the form factors at maximum recoil. The two complementary constraints can be merged together in pole dominance ansätze for the form factors, where the crucial property is the order of the pole. Lattice calculations can be used to verify these ansätze. In practice, it is easier to measure

form factors near $q^2_{\rm max}$ in experiments, and near $q^2 = 0$ on the lattice. The pole dominance ansätze are often conveniently adopted to extend them to other q^2.

Lattice calculations can observe how the symmetry relations amongst the form factors get modified as the quark masses are reduced. For the semileptonic pseudoscalar-to-pseudoscalar decay, the pole relation between f_+ and f_0 is well satisfied, even when the the heavy quark mass is $\mathcal{O}(m_c)$, as exemplified in Fig.9 [18]. The $\mathcal{O}(M^{-1})$ corrections to the relations amongst the form factors appearing in the semileptonic pseudoscalar-to-vector decay are larger, in particular the relation between V and A_1 works poorly even at m_b. The corrections seem to affect mostly the normalisations, however, and not the q^2-dependence. The form factors occuring in the radiative decay $B \to K^*\gamma$, and heavy-to-light semileptonic decays $B \to \rho l\nu$ and $B \to \pi l\nu$, can be related using heavy quark and light flavour $SU(3)$ symmetries. These relations seem to work well, but the q^2-dependence of the form factors is not yet fully sorted out in lattice calculations [16, 19].

The Isgur-Wise functions have been extracted from lattice form factors evaluated at sufficiently heavy quark mass. Examples for meson and baryon cases are shown in Fig.10 [18] and Fig.11 [20] respectively. The meson Isgur-Wise function, $\xi(v_i \cdot v_f)$, shows an increase as the light quark mass is reduced, and the slope at zero recoil is $\xi'(1) \approx -1$ in the chiral limit. First results for the baryon Isgur-Wise function [20] indicate that it falls off more steeply than the meson one, and its slope decreases by about a factor of two between m_s and the chiral limit.

In strong coupling lattice QCD, $\xi(v_i \cdot v_f)$ has a double pole form, with the singularity at $v_i \cdot v_f = -1$ [21]. This result can be rephrased as PCVC: the divergence of the partially conserved vector current is saturated by the scalar meson pole near $M_i + M_f$ (the scalar pole may arise from the combination of a set of states spread over an energy range much smaller than M). This ansatz fits both the lattice and experimental (Fig.12 [22] shows the latest results) data as well as any other fit. It is worth exploring if there is any limit of QCD, quite likely it would involve $N_c \to \infty$, where this ansatz becomes exact.

VI. CONSTRAINING THE STANDARD MODEL

Lattice results can help in precision tests of the standard model, by pinning down the elements of the Cabbibo-Kobayashi-Masakwa quark mixing matrix. Of particular interest is the unitarity triangle involving the third generation, which determines $CP-$violation. The present constraints can best be expressed in terms of the Wolfenstein parameters ρ and η, and they are displayed in Fig.13. Particularly useful here are the lattice inputs for f_B, B_B and B_K [23]. The bounds suggest that, within the standard model, $CP-$violation is close to maximal (i.e. the phase $\delta \sim \pi/2$). The standard model will be constrained further by results leading to $|\epsilon'/\epsilon|$.

Lattice f_B, B_B values also determine, in terms of $|V_{ts}|$, the extent of $B_s - \overline{B_s}$ oscillations. These oscillations may be observable at LEP, SLC and HERA-B [19].

Acknowledgements: I thank the organisers for an informative and enjoyable workshop. I am grateful to the Physics Department, University of Wuppertal for its hospitality during the completion of this review.

References

[1] Review of Particle Properties, Phys. Rev. D54 (1996) 1.

[2] Proceedings of LATTICE 95, Nucl. Phys. B (Proc. Suppl.) 47 (1996).

[3] Proceedings of LATTICE 96, Nucl. Phys. B (Proc. Suppl.), to appear.

[4] G.P. Lepage, L. Magnea, C. Nakhleh, U. Magnea and K. Hornbostel, Phys. Rev. D46 (1992) 4052.

[5] J. Shigemitsu, in Ref.[3], hep-lat/9608058.

[6] G.P. Lepage, in Ref.[2], p.3, hep-lat/9510049.

[7] G. Bodwin, S. Kim and D. Sinclair, hep-lat/9605023.

[8] G. Bodwin, E. Braaten and G.P. Lepage, Phys. Rev. D51 (1995) 1125.

[9] P. Weisz, in Ref.[2], p.71, hep-lat/9511017.

[10] P. McCallum and J. Shigemitsu (NRQCD collaboration), in Ref.[2], p.409, hep-lat/9510006.

[11] B. Grinstein and I. Rothstein, Phys. Lett. B385 (1996) 265, hep-ph/9605260.

[12] C. Bernard et al. (MILC collaboration), in Ref.[3], hep-lat/9608088.

[13] S. Collins (SGO collaboration), in Ref.[3], hep-lat/9608064.

[14] S. Hashimoto et al. (JLQCD collaboration), in Ref.[3], hep-lat/9608142.

[15] V. Giménez, G. Martinelli and C.T. Sachrajda, in Ref.[3], hep-lat/9608039.

[16] J. Flynn, in Ref.[3], hep-lat/9610010.

[17] For a review, see M. Neubert, Phys. Rep. 245 (1994) 259.

[18] T. Bhattacharya and R. Gupta, in Ref.[2], p.481, hep-lat/9512007.

[19] A. Soni, in Ref.[2], p.43, hep-lat/9510036.

[20] N. Stella et al. (UKQCD collaboration), in Ref.[3], hep-lat/9607072.

[21] A. Patel, in proceedings of the International Colloquium on Modern Quantum Field Theory II, Bombay, 1994, eds. S. Das and G. Mandal, World Scientific (1995), p.317, hep-ph/9405213.

[22] B. Barish et al. (CLEO Collaboration), Phys. Rev. D51 (1995) 1014;
T. Browder and K. Honscheid, Prog. Part. Nucl. Phys. 35 (1995) 81.

[23] S.R. Sharpe, in Ref.[3], hep-lat/9609029.

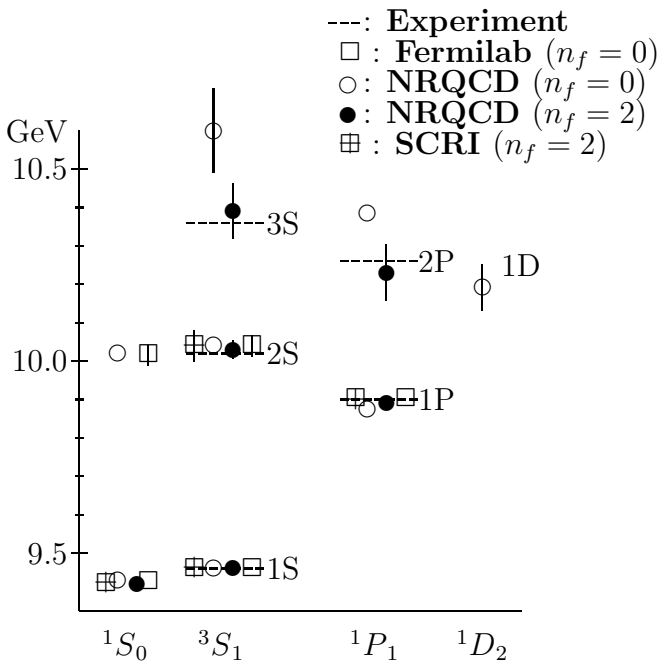

Figure 1: Υ spin-averaged spectrum [5].

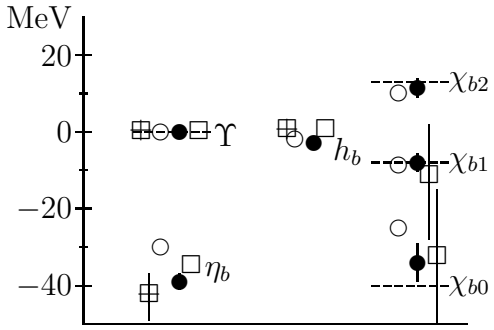

Figure 2: Υ spin-splittings [5]. The symbols have the same meaning as in Fig.1.

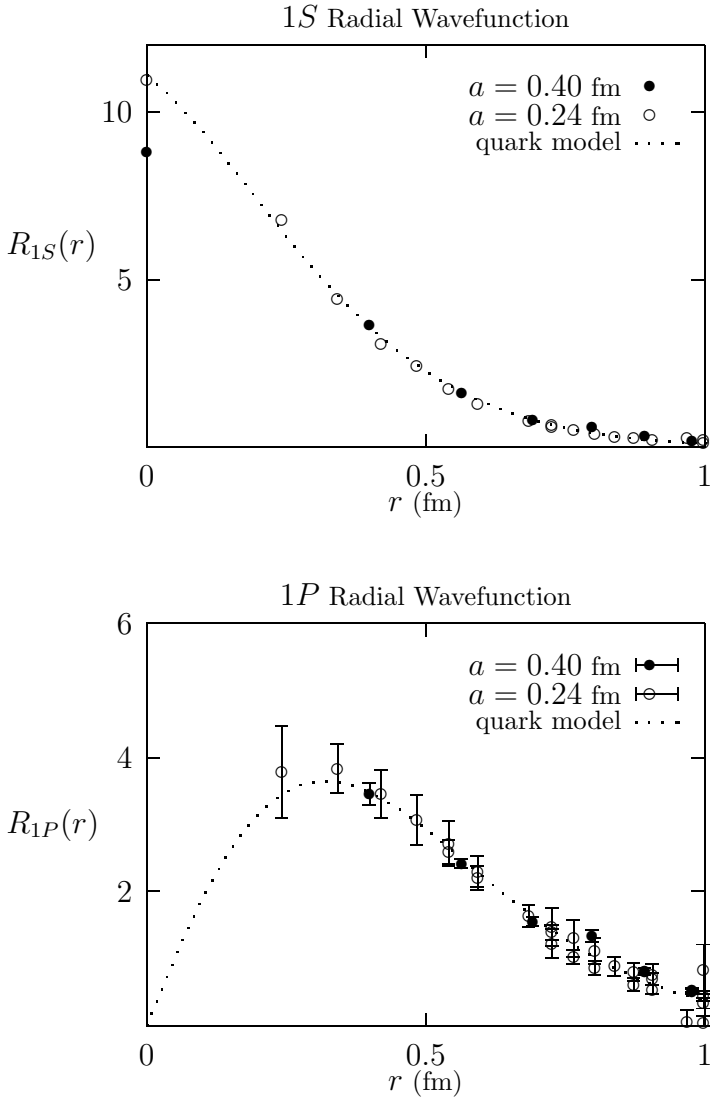

Figure 3: The radial wavefunctions for the $1S$ and $1P$ Charmonium states computed using improved actions and two different lattice spacings [6]. Wavefunctions from a continuum quark model are also shown. Statistical errors are negligible for the $1S$ wavefunction.

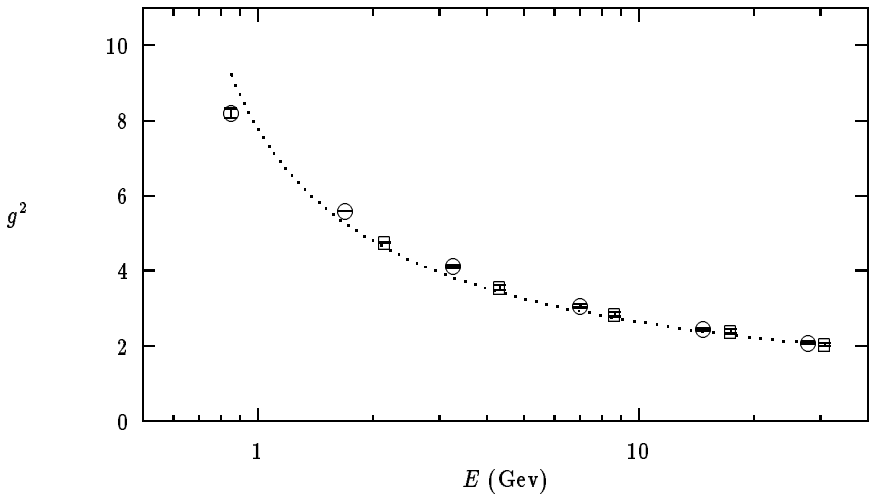

Figure 4: A comparison of the pure gauge $SU(2)$ running coupling for two different non-perturbative definitions [9]: squares are g^2_{SF} and circles are g^2_{TP}. The energy scales have been matched with the appropriate ratio of the $\Lambda-$parameters. The dotted line shows the perturbative 2−loop evolution.

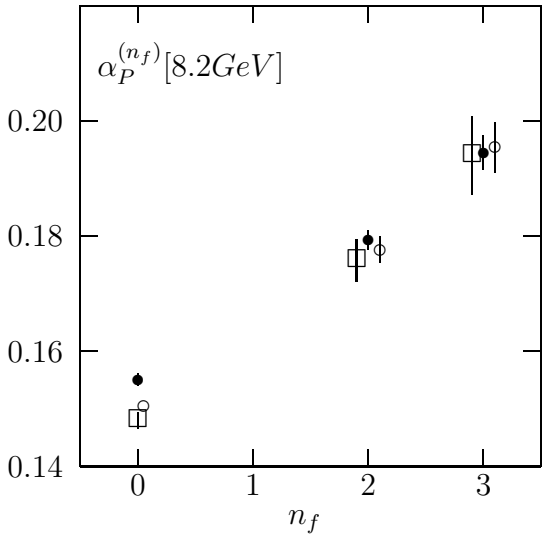

Figure 5: $\alpha_P^{(n_f)}[8.2GeV]$ versus n_f [10]. The scale is set by the Υ 1S-1P (full circles), the Υ 1S-2S (open circles) or the Charmonium 1S-1P (boxes) splitting.

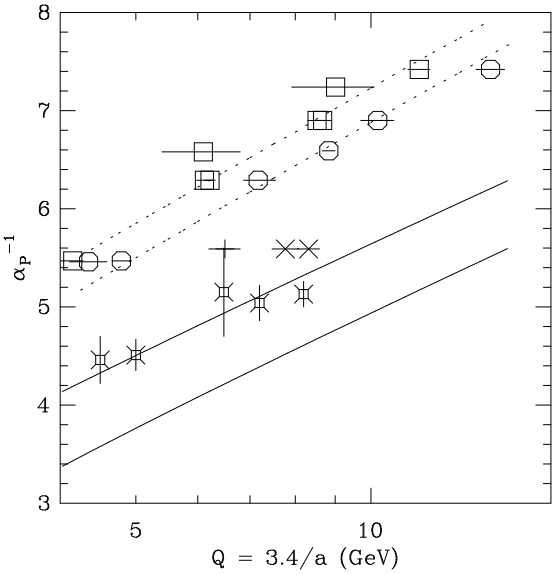

Figure 6: α_P^{-1} versus $\ln(\frac{3.4}{a})$ [5]. The symbols are: $n_f = 0$ charm ($\Box$), $n_f = 0$ bottom ($\bigcirc$), $n_f = 2$ charm ($+$), $n_f = 2$ bottom ($\times$), and $n_f = 3$ extrapolated (fancy boxes). The region between the two full curves corresponds to $\alpha_{\overline{MS}}(M_Z) \in [0.115, 0.125]$, typically obtained in non-lattice determinations. The dotted lines are 3−loop scaling curves for $n_f = 0$.

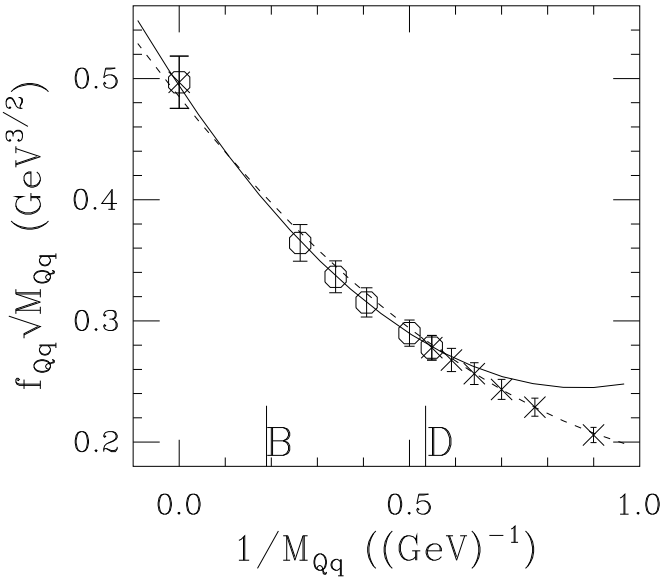

Figure 7: $f_{Qq}(M_{Qq})^{\frac{1}{2}}$ vs. $1/M_{Qq}$ for $n_f = 0$, $\beta = 6.3$ Wilson fermions [12]. The solid line is a quadratic fit to the octagons ("heavier heavies" + static); the dashed line is a quadratic fit to the crosses ("lighter heavies" + static).

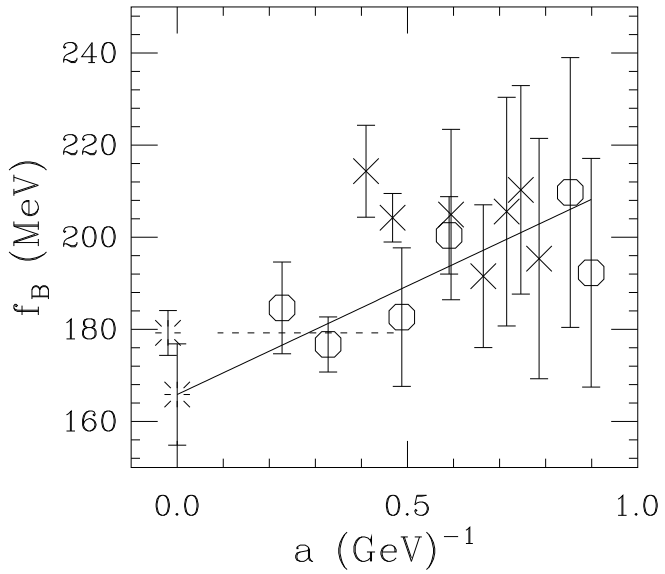

Figure 8: f_B vs. a for $n_f = 0$ (octagons) and $n_f = 2$ (crosses) data [12]. The solid line is a linear fit to all $n_f = 0$ points; the dashed line is a constant fit to the three $n_f = 0$ points with $a < 0.5$ GeV^{-1}. The extrapolated values at $a = 0$ are indicated by bursts. The scale is set by $f_\pi = 132$ MeV throughout.

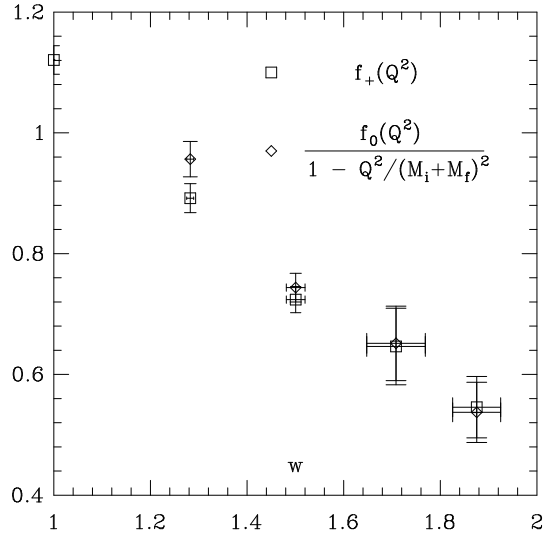

Figure 9: Comparison of semileptonic decay form factors for the heavy-light pseudoscalar meson [18]. The heavy quark mass roughly changes from m_c to m_s, while the light quark mass is about $0.4m_s$.

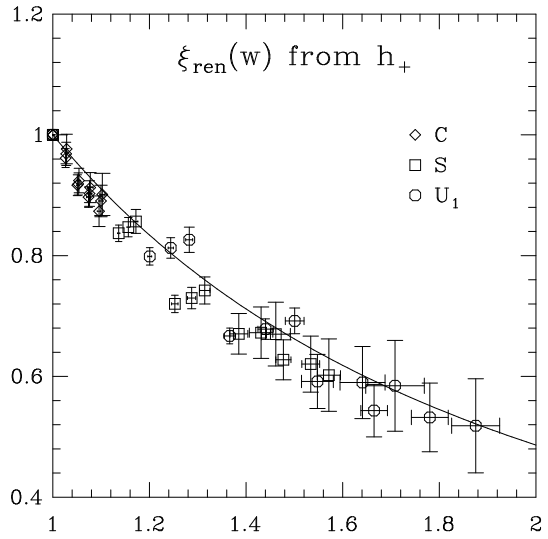

Figure 10: $\xi(w)/\xi(1)$ at various quark masses [18]. The initial heavy quark mass is about m_c, and various symbols label the masses it decays into (from m_c to m_s). The clusters of three points show an increase in the form factor with a decrease in the spectator quark mass (from m_s to $0.4m_s$).

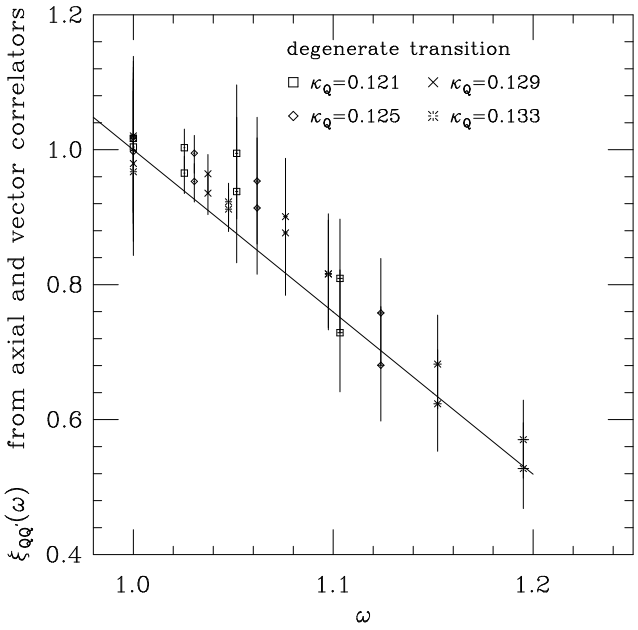

Figure 11: The baryon Isgur-Wise function from the elastic form factor [20]. Different symbols denote different heavy quark massess in the vicinity of m_c, while the light quark masses straddle m_s. The points with the same ω depict an increase in the form factor with a decrease in the spectator quark masses.

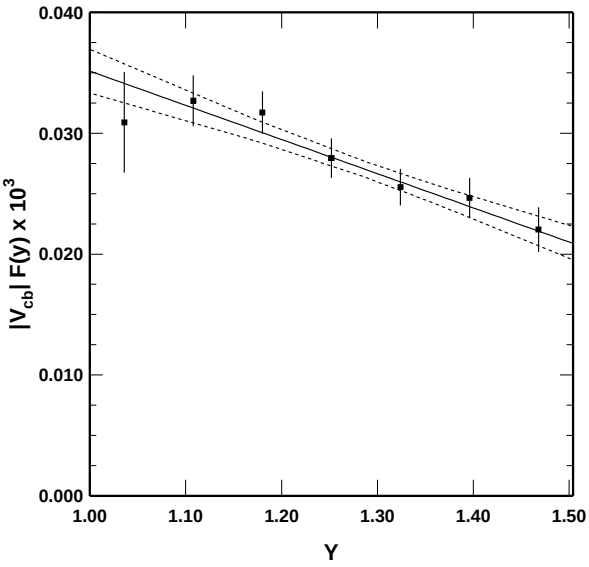

Figure 12: The $\bar{B} \to D^* l \bar{\nu}$ form factor from CLEO II [22]. $y = v_i \cdot v_f$ and $F(y)$ reduces to the Isgur-Wise function in the limit $m_b, m_c \to \infty$. Combination of ARGUS, CLEO II and ALEPH results, with the latest world average lifetimes [1], gives the linear fit parameters: $V_{cb}F(1) = 0.0359(22)$ and slope $\hat{\rho}^2 = 0.88(12)$.

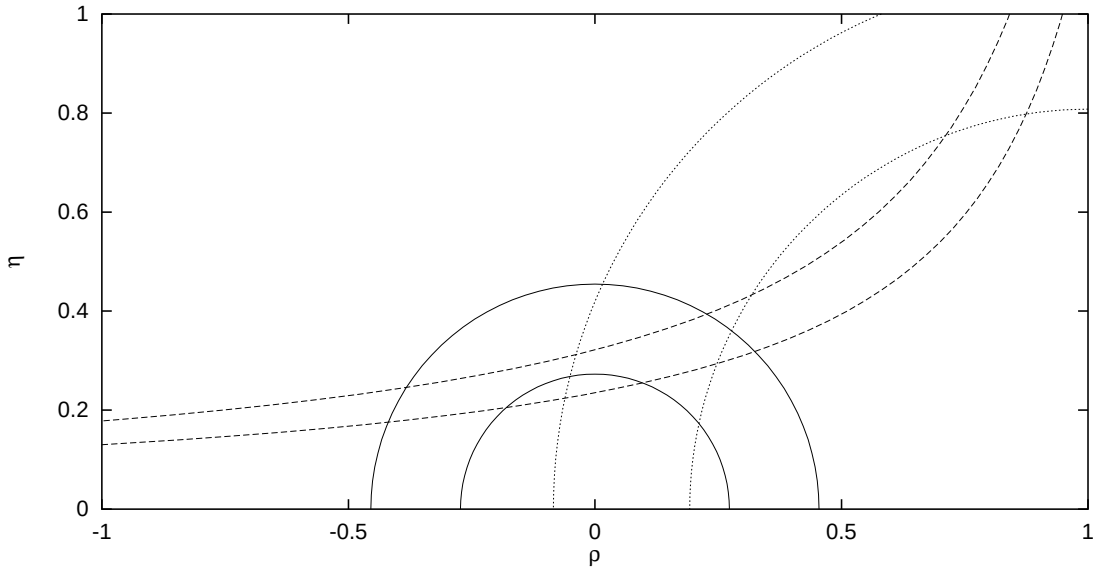

Figure 13: Constraints on the Wolfenstein parameters of the quark mixing matrix, from the combination of current experimental [1] and lattice results. The solid semi-circles are from $|V_{ub}/V_{cb}|$, the dashed hyperbolas are from $|\epsilon|$ and B_K, and the dotted circles are from Δm_B and $f_B^2 B_B$.